J IRAN CHEM SOC
DOI 10.1007/s13738-016-1020-x

ORIGINAL PAPER

A new palladium complex supported on magnetic nanoparticles and applied as an catalyst in amination of aryl halides, Heck and Suzuki reactions

Arash Ghorbani-Choghamarani[1] · Bahman Tahmasbi[1] · Nourolah Noori[1] · Raziyeh Ghafouri-nejad[1]

Received: 11 July 2016 / Accepted: 24 November 2016

Abstract A simple, efficient and less expensive protocol for the phosphine-free C–C coupling reactions and synthesis of anilines in the presence of 2-aminobenzamide complex of palladium supported on Fe_3O_4 magnetic nanoparticles (Pd(0)-ABA-Fe_3O_4) has been reported. The Suzuki reaction was carried out in water or PEG using phenylboronic acid ($PhB(OH)_2$) or sodium tetraphenyl borate ($NaBPh_4$). Pd(0)-ABA-Fe_3O_4 has been found promising for Heck reaction of butyl acrylate, styrene or acrylonitrile with aryl halides (including Cl, Br and I). Also, Pd(0)-ABA-Fe_3O_4 has been found as efficient catalyst for the amination of aryl halides using aqueous ammonia. The products have been obtained in short reaction times and high yields. The catalyst was easily separated using an external magnet from the reaction mixture and reused for several runs without significant loss of its catalytic efficiency or palladium leaching. The leaching of catalyst has been examined by hot filtration and ICP-OES technique. The nanomagnetical catalyst was characterized by FTIR, TGA, XRD, VSM, TEM, SEM, EDS, DLS and ICP-OES techniques.

Keywords Magnetic nanoparticle · Palladium · Amination · Heck reaction · Suzuki reaction

Introduction

The formation of carbon–carbon bond via Heck and Suzuki reaction has been frequently employed in the synthesis of natural products, agrochemicals, pharmaceuticals, biologically active compounds and advanced materials [1, 2]. The Suzuki cross-coupling reaction is one of the most general and powerful tools for the synthesis of pharmaceuticals, herbicides, polymers, liquid crystals, natural products, ligands for catalysis and advanced materials [3, 4]. Traditionally, the carbon–carbon bond forming reactions are carried out in organic solvents in the presence of palladium complexes including organic ligands at high temperatures [5]. However, there are some disadvantages accompany with these procedures. First of all, the employed organic solvents may cause serious environmental problems due to their toxicity, and the reactions carried out at higher temperatures definitely consume more energy [6]. Secondly, the most common catalytic system employed for C–C coupling reaction is promoted by homogeneous palladium complexes containing ligands such as phosphine, dibenzylideneacetone and carbenes, which the preparation of most of the homogeneous Pd complexes with air- and moisture-sensitive phosphine and expensive ligands, leading to high production cost, reuse of these catalysts is difficult; moreover, they are environmentally malignant [7, 8]. Therefore, the immobilization of homogeneous catalysts on various support materials to combine the advantages of both homogeneous and heterogeneous catalysis such as high catalytic activity, easily recyclable, moisture- and air-stable catalyst is of great importance in catalyst science [9–11]. Meanwhile, some of the previously heterogeneous supports such as MCM-41 [28], SBA-15 [12] or some nanoparticles such as TiO_2 NPs [13] require high temperature for calcination or a lot of time and tedious condition to prepare. Also, some of these reported catalysts such as heteropolyacids [14], carbon nanotubes [10], ionic liquids [15] or some polymers [16] are more expensive. In addition, most common heterogeneous catalyst can be separated from products by conventional techniques, which has some disadvantages such

✉ Arash Ghorbani-Choghamarani
arashghch58@yahoo.com; a.ghorbani@mail.ilam.ac.ir

[1] Department of Chemistry, Ilam University, P.O. Box 69315516, Ilam, Iran

Published online: 28 November 2016

as time-consuming and expensive separation of fine particles from a reaction mixture [17]. Fe_3O_4 MNPs were prepared in water using commercially available materials such as $FeCl_3{\cdot}4H_2O$ and $FeCl_2{\cdot}4H_2O$. Furthermore, magnetic nanoparticles (MNPs) can be easily and rapidly separated from the reaction mixture with the assistance of an external magnet [18, 19]. More important, magnetic separation of the MNPs is more effective and easier than filtration or centrifugation. In the other hand, MNPs are readily available, insoluble in organic and aqueous solvents and high surface area resulting in high catalysts loading capacity and outstanding stability heterogeneous supports for catalyst [20–22]. Recently, much attention has been focused on the surface modification with appropriate capping agents onto the MNPs surface to anchor the catalytically active complexes [9, 20, 23]. The Pd/H_2N/Fe_3O_4 catalyst provides excellent reactivity and reusability in the C–C coupling reactions [23]. Typically, Suzuki reactions involve palladium catalyzed cross-coupling between aryl halides and organoboronic compounds such as trifluoroborates, organoboranes, boronic esters and boronic acid derivatives [24]. These advantages are based on the properties of the air- and moisture-stable organoboron nucleophiles, which can be easily obtained by a variety of synthetic routes and have low toxicity [25]. Also, the Heck reaction is one of the most powerful and versatile method for the coupling of aryl halides with olefins. Heck reaction is normally catalyzed by Pd complexes in the presence of base for the formation of C–C bonds [16].

Amination of aryl halides is a very important transformation and a method for the synthesis of anilines. Anilines are important building blocks for the constructing natural products, pharmaceutical and medicinal compounds, as well as in polymers and materials [26, 27]. Recently, few groups have reported several catalytic systems for the direct conversion of aryl halides into anilines [27–29]. Among them, ammonia is used as one of the most attractive sources of nitrogen for the synthesis of anilines because of its inexpensive cost and wide availability [30]. Thus, the development of efficient method for the amination of aryl halides is highly desirable. Owing to the inherent advantages of recovery, in the context of reuse of palladium, herein a new Pd-based heterogeneous catalyst has been reported for the C–C coupling reactions and synthesis of anilines from aryl halides.

Experimental

Preparation of the catalyst

Fe_3O_4 MNPs were prepared using chemical precipitation of ions Fe^{3+} and Fe^{2+} with a molar ratio of 2:1. Typically, $FeCl_3{\cdot}6H_2O$ (5.838 g) and $FeCl_2{\cdot}4H_2O$ (2.147 g) were dissolved in 100 mL deionized water at 80 °C under N_2 atmosphere and vigorous mechanical stirring conditions. Then, 10 mL of 25% NH_4OH was added to the reaction mixture. After 30 min, the mixture of reaction was cooled to room temperature. After completion of the reaction, nanoparticles (Fe_3O_4) were washed two times with distilled water and 0.02 M solution of NaCl, and each time was decanted with external magnet.

Fe_3O_4 nanoparticles (1.5 g) were dispersed in 50 mL ethanol/water (volume ratio, 1:1) solution by sonication for 30 min, and then, APTES (2.5 mL) was added to the mixture reaction. The reaction mixture was stirred under N_2 atmosphere at 40 °C for 8 h. Then, the nanoparticles was re-dispersed in ethanol by sonication for 5 times and separated through magnetic decantation. The nanoparticles (NH_2–MNPs) were dried at room temperature. The obtained NH_2–Fe_3O_4 nanoparticles (1 g) were dispersed in 50 mL ethanol by sonication for 30 min, and then, isatoic anhydride (2.5 mmol) was added to the reaction mixture. The reaction mixture was stirred under N_2 atmosphere at 80 °C for 8 h. Then, the reaction mixture was cooled down to room temperature, and the resulting nanoparticles washed with ethanol for several times and separated using magnetic decantation and dried at room temperature. The obtained ABA-Fe_3O_4 (0.5 g) was dispersed in 25 mL ethanol by sonication for 30 min, and then, palladium acetate (0.25 mmol) was added to the reaction mixture. The reaction mixture was stirred under N_2 atmosphere at 80 °C for 20 h. Then, the $NaBH_4$ (0.3 mmol) was added to the reaction mixture and stirred for 2 h. Then, the final product was separated by magnetic decantation and washed by ethanol to remove the unattached substrates. The nanoparticles product (Pd(0)-ABA-Fe_3O_4) was dried at room temperature.

General procedure for C–C coupling reaction using sodium tetraphenyl borate

A mixture of aryl halide (1 mmol), sodium tetraphenyl borate (0.5 mmol), Na_2CO_3 (3 mmol) and Pd(0)-ABA-Fe_3O_4 (0.01 g, 1.85 mol%) was stirred in PEG at 80 °C and the progress of the reaction was monitored by TLC. After completion of the reaction, the mixture was cooled to room temperature and catalyst was separated by an external magnet and washed with diethyl ether and the reaction mixture was extracted with H_2O and diethyl ether. The organic layer was dried over Na_2SO_4 (1.5 g). Then, the solvent was evaporated and pure biphenyl derivatives were obtained in good to excellent yields.

General procedure for coupling of aryl halides with phenylboronic acid (Suzuki reaction)

A mixture of aryl halide (1 mmol), phenylboronic acid (1 mmol), Et_3N (3 mmol) and Pd(0)-ABA-Fe_3O_4 (0.003 g,

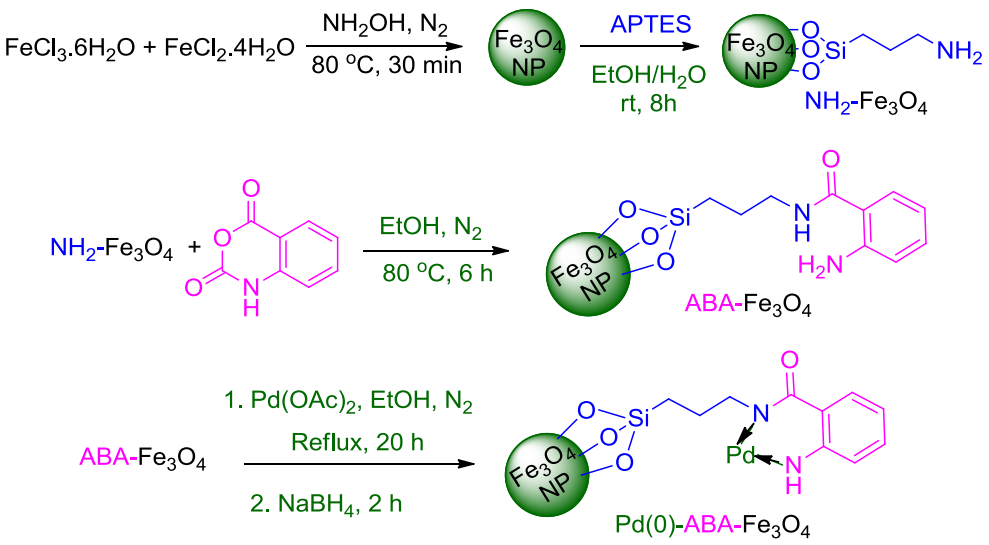

Scheme 1 Synthesis of Pd(0)-ABA-Fe_3O_4 nanoparticles

0.56 mol%) was added to a reaction vessel. The resulting mixture was stirred in H_2O at room temperature, and the progress of the reaction was monitored by TLC. After completion of the reaction, catalyst was separated by an external magnet and washed with ethylacetate and the reaction mixture was extracted with H_2O and ethylacetate and dried over anhydrous Na_2SO_4 (1.5 g). Then, the solvent was evaporated and pure biphenyl derivatives were obtained in good to excellent yields.

General procedure for coupling of aryl halides with butyl acrylate, acrylonitrile or styrene (Heck reaction)

A mixture of aryl halide (1 mmol), alkene (1.2 mmol), K_2CO_3 (3 mmol), and Pd(0)-ABA-Fe_3O_4 (0.008–0.016 g, 1.48–2.96 mol%) was stirred in DMF at 120 °C, and the progress of the reaction was monitored by TLC. After completion of the reaction, the mixture was cooled to room temperature and catalyst was separated by an external magnet and washed with diethyl ether and the reaction mixture was extracted with H_2O and diethyl ether. The organic layer was dried over Na_2SO_4 (1.5 g). Then, the solvent was evaporated and pure products were obtained in 95–98% yields.

General procedure for amination of aryl halides

Aryl halide (1 mmol) was added to a mixture of the catalyst (10 mg, 1.85 mol%), K_2CO_3 (3 mmol) and NH_4OH (1 mL) and stirred at 60 °C. The progress of the reaction was monitored by TLC. After the completion of the reaction, catalyst was separated using an external magnet. Then, gathered aqueous phases were extracted with ethyl acetate. The organic layer was dried over Na_2SO_4 and then evaporated under reduced pressure, aniline derivatives have been obtained in good yields.

Results and discussion

Catalyst preparation

The *N*-propylamine supported on Fe_3O_4 MNPs (NH_2–Fe_3O_4) core shell was synthesized by a modified new reported procedure [31], and then, 2-aminobenzamide immobilized on Fe_3O_4 (ABA-Fe_3O_4) has been prepared by reaction of NH_2–Fe_3O_4 with isatoic anhydride. Finally, 2-aminobenzamide complex of Pd supported on Fe_3O_4 (Pd(0)-ABA-Fe_3O_4) has been obtained via reaction of palladium(II) acetate and ABA-Fe_3O_4 (Scheme 1). This catalyst has been characterized by transmission electron microscopy (TEM), scanning electron microscopy (SEM), energy-dispersive X-ray spectroscopy (EDS), X-ray diffraction (XRD), thermogravimetric analysis (TGA), vibrating sample magnetometer (VSM), Fourier transform infrared spectroscopy (FTIR), dynamic laser scattering (DLS) and inductively coupled plasma atomic emission spectroscopy (ICP-OES).

Catalyst characterizations

The morphology and size of the catalyst was evaluated by SEM and TEM analysis (Fig. 1). Transmission electron microscopy was used to obtain direct information about the size and morphology of the prepared nanoparticles. It can be seen that most of the particles are quasi-spherical

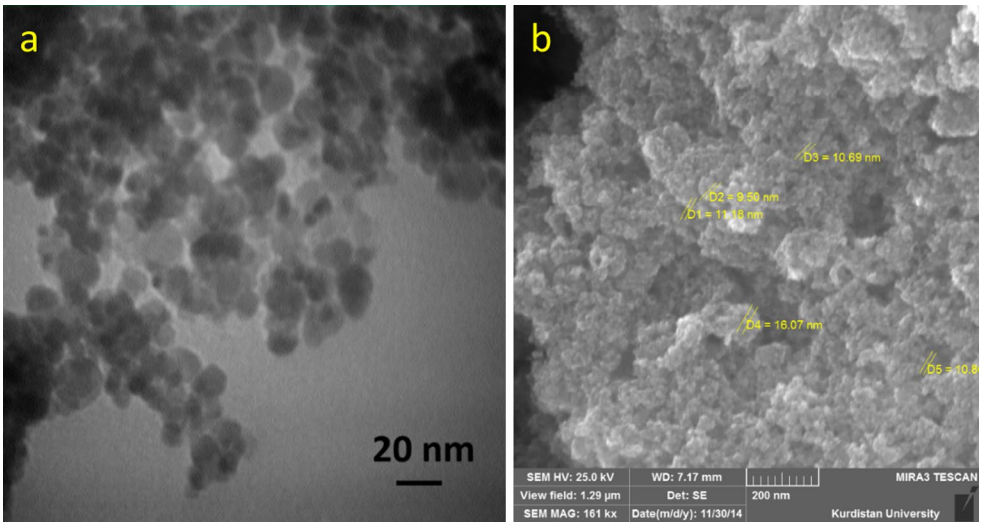

Fig. 1 TEM (**a**) and SEM (**b**) image of Pd(0)-ABA-Fe_3O_4

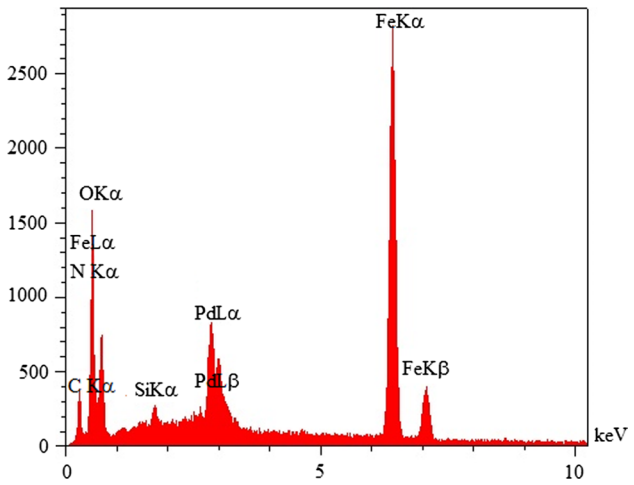

Fig. 2 EDX spectrum of Pd(0)-ABA-Fe_3O_4

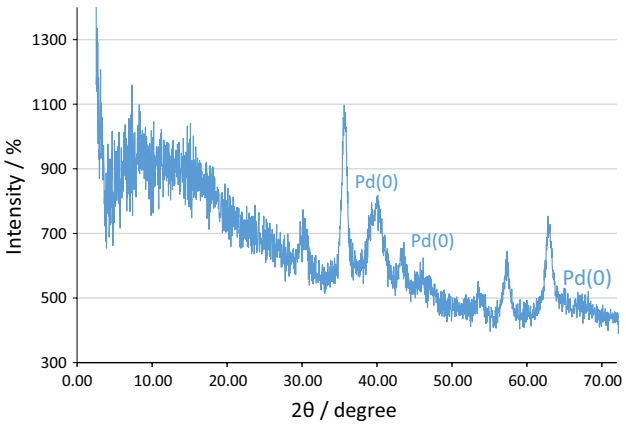

Fig. 3 XRD pattern of Pd(0)-ABA-Fe_3O_4

with an average diameter about 15–25 nm. Also, the size and morphology of Pd(0)-ABA-Fe_3O_4 is quite homogeneous with obtained diameter of 15–20 nm. To investigate the size distribution of these nanoparticles, particles size was calculated by SEM analysis, which the catalyst was formed of nanometer-sized particles as shown in SEM image. A typical EDS spectrum taken from the Pd(0)-ABA-Fe_3O_4 is shown in Fig. 2. The EDS spectra at different points of the image confirm the presence of Pd in the prepared modified nanoparticles. As shown in this figure, EDS spectrum of catalyst showed the presence of C, N, O, Si, Fe and Pd species in the catalyst (Fig. 2).

Also, to extend the scope of catalysts characterization, we have determined the exact amount of Pd on MNPs by ICP-OES technique. The Pd amount of the immobilized catalyst on MNPs was found to be 1.85×10^{-3} mol g^{-1} based on inductively coupled plasma atomic emission spectroscopy (ICP-OES).

The XRD pattern of Pd(0)-ABA-Fe_3O_4 is shown in Fig. 3. As it is shown in Fig. 3, Pd(0)-ABA-Fe_3O_4 displays six characteristic peaks at the 2θ values of 30.18, 35.64, 43.62, 54.02, 57.35 and 63.09 which could be attributed for the (220), (311), (400), (422), (511) and (440) reflections, respectively, which were in agreement with magnetite standard data. Weak broad bands ($2\theta < 20°$) appeared in XRD pattern which could be attributed to the amorphous silane shell formed around the magnetic cores [32]. Also, the XRD pattern of Pd(0)-ABA-Fe_3O_4 contains a series of characteristic diffraction peaks (39.8°, 46.3° and 67.8°) which are indexed to the Pd indicating the presence of Pd on surface of magnetic nanoparticles [33].

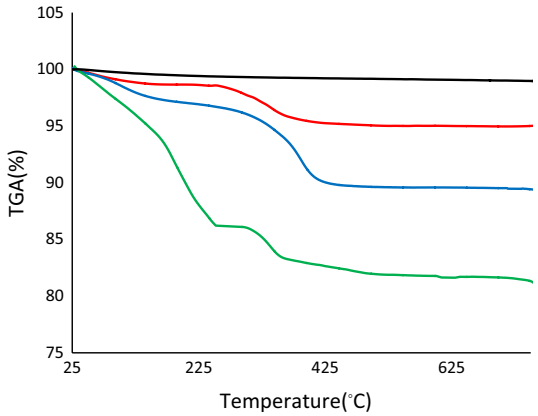

Fig. 4 TGA diagram of Fe_3O_4 MNPs (*black line*), NH_2–Fe_3O_4 (*red curve*), ABA-Fe_3O_4 (*blue curve*) and Pd(0)-ABA-Fe_3O_4 (*green curve*)

The average size of Pd(0)-ABA-Fe_3O_4 nanocatalyst diameter was calculated to be 21 ± 1.2 nm from the XRD results by Scherrer's equation:

$$D = k\lambda/\beta\cos\theta$$

where D is the average particle size of the phase under investigation, k is Scherrer's constant (0.9), λ is the applied wavelength (1.5405 Å), β is the corrected diffraction line full width at half-maximum (FWHM), applied to the principal diffraction peak corresponding to the plane (3 1 1) and θ is the angle of diffraction.

One indication of bond formation between the nanoparticles and the complex can be inferred from TGA. The TGA curve of the Pd(0)-ABA-Fe_3O_4 shows the mass loss of the organic functional groups as it decomposes upon heating. Figure 4 shows the TGA curves for bare Fe_3O_4 nanoparticles (black curve), NH_2–Fe_3O_4 (red curve), 2-aminobenzamide supported on Fe_3O_4 magnetic nanoparticle (ABA-Fe_3O_4) (blue curve) and the catalyst treated nanoparticles (green curve). The TGA curve of the all samples shows the small amount of weight loss below 200 °C is due to desorption of physically adsorbed solvents and surface hydroxyl groups. In TGA curve of the catalyst, a weight loss about of 20% from 200 to 500 °C, resulting from the decomposition of immobilized organic spaces on the Fe_3O_4 surface. Meanwhile, weight loss about 5 and 10% from 200 to 500 °C is occurred for NH_2–Fe_3O_4 and ABA-Fe_3O_4, respectively. On the basis of this result, the well grafting of organic groups including palladium complex on the Fe_3O_4 is verified.

The dynamic laser scattering measurement of Pd(0)-ABA-Fe_3O_4 nanoparticle is shown in Fig. 5. The hydrodynamic diameter of the nanoparticles in water was found to be monodisperse with mean values of 48.8 nm, slightly larger than observed from TEM and XRD report due to the effect of agglomeration of nanoparticles, solvation and the

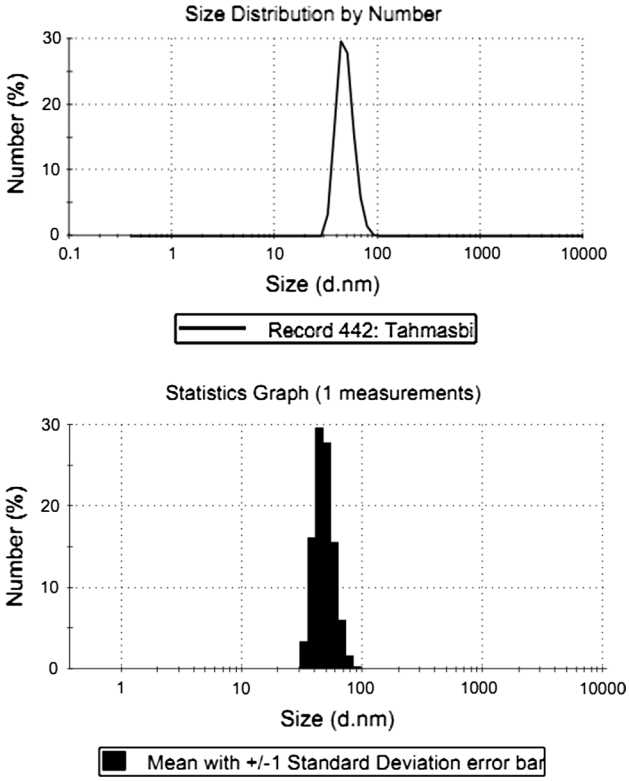

Fig. 5 Dynamic laser scattering measurement of Pd(0)-ABA-Fe_3O_4

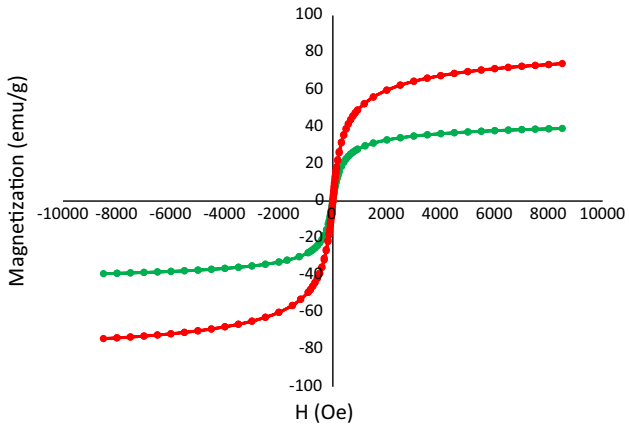

Fig. 6 Magnetization curves for Fe_3O_4 (*red line*) and Pd(0)-ABA-Fe_3O_4 (*green line*) at room temperature

presence of organic layers and Pd complex immobilized on the surface of Fe_3O_4 nanoparticles.

The magnetic property of Fe_3O_4 nanoparticles and Pd(0)-ABA-Fe_3O_4 was characterized by VSM. The room-temperature magnetization curves of Fe_3O_4 MNPs and Pd(0)-ABA-Fe_3O_4 are shown in Fig. 6. The magnetic measurement shows that the Pd(0)-ABA-Fe_3O_4 has a saturated magnetization value of 38.9 emu g^{-1}. As expected, the

Fe_3O_4 nanoparticles showed the higher magnetic value (saturation magnetization, Ms) of 74.1 emu g^{-1} [18], and the Ms value of Pd(0)-ABA-Fe_3O_4 is decreased due to the silica coating and the layer of the grafted catalyst (39.1 emu g^{-1}).

Successful functionalization of the Fe_3O_4 MNPs can be inferred from FTIR technique. The FTIR spectrum for bare Fe_3O_4 nanoparticles (a), NH_2–Fe_3O_4 (b), ABA-Fe_3O_4 (c) and Pd(0)-ABA-Fe_3O_4 (d) is shown in Fig. 7. The FTIR spectrum of Pd(0)-ABA-Fe_3O_4 shows several peaks that are characteristic of a functionalized palladium complex, which clearly differs from that of the unfunctionalized bare Fe_3O_4, NH_2–Fe_3O_4 and ABA-Fe_3O_4 nanoparticles. The FTIR spectrum for the Fe_3O_4 shows a stretching vibration at 3393 cm^{-1} which incorporates the contributions from both symmetrical and asymmetrical modes of the O–H bonds which are attached to the surface magnetic nanoparticles. The strong band at low wavenumbers (562 cm^{-1}) comes from the vibrations of Fe–O bonds of iron oxide [6]. In the FTIR spectra of NH_2–Fe_3O_4, the presence of the anchored *N*-propylamine group is confirmed by C–H stretching vibrations that appear at 2924 and 2856 cm^{-1} and also N–H stretching vibration modes as a broad band that appear at 3440 cm^{-1} [1]. More importance, the Fe–O–Si stretching vibrations and both symmetrical and asymmetrical modes of the O–Si as a broad band appear between 1000 and 1100 cm^{-1}, which indicates that the silica organic group has successfully coated on the surface of Fe_3O_4 nanoparticles [19, 34]. Reaction of isatoic anhydride with *N*-propylamine produces ABA-Fe_3O_4 in which the presence of carbonyl group is asserted with 1625 cm^{-1} bands in FTIR spectra (Fig. 7c). Also, vibrations at 1450 cm^{-1} and vibration at 1525 cm^{-1} were probably attributed to the terminal amine groups and ring attached C–N, respectively [7]. In addition, in the spectrum of Pd(0)-ABA-Fe_3O_4, the broadening in the range of 1400–1650 cm^{-1} is attributed to the formation of palladium complex. All of those bands reveal that the surface of Fe_3O_4 nanoparticles is successfully modified with organic layers.

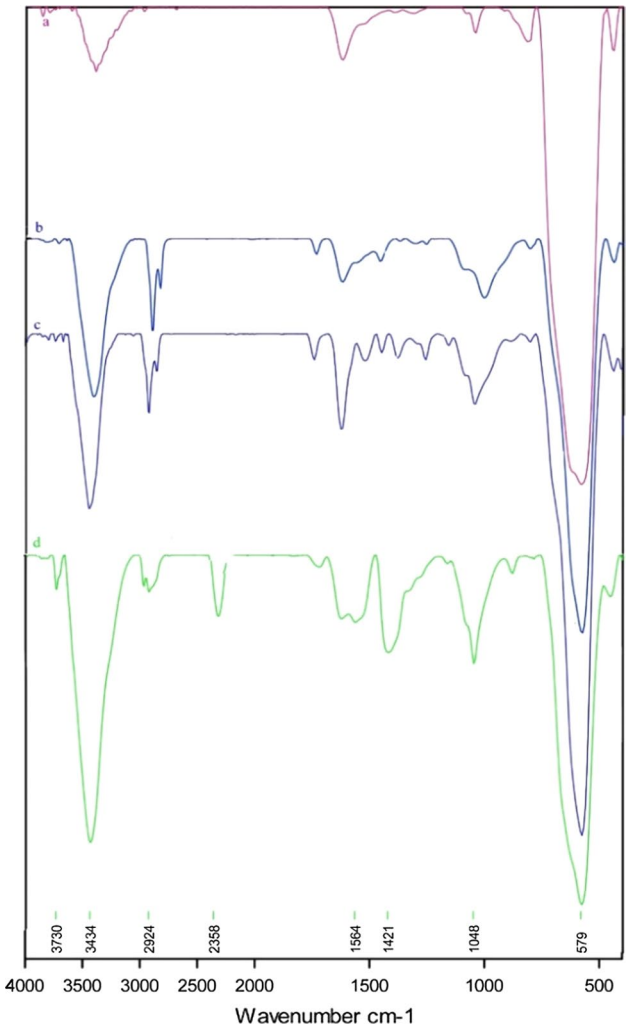

Fig. 7 FTIR spectrums of Fe_3O_4 MNPs (*a*), NH_2–Fe_3O_4 (*b*), ABA-Fe_3O_4 (*c*) and Pd(0)-ABA-Fe_3O_4 (*d*)

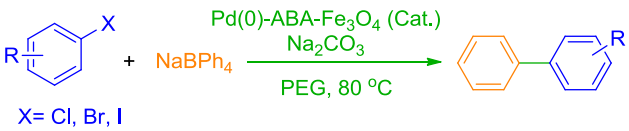

Scheme 2 Carbon–carbon coupling reaction using sodium tetraphenyl borate in the presence of Pd(0)-ABA-Fe_3O_4

Catalytic studies

As a part of our ongoing program directed toward the catalytic activity of modified nanoparticles in organic reactions [35–37], we were interested in finding a simple and efficient method for the carbon–carbon coupling reaction in the presence of magnetic nanoparticles bonded palladium complex (Pd(0)-ABA-Fe_3O_4) as a magnetically recoverable nanocatalyst (Scheme 2).

To illustrate the catalytic activity of Pd(0)-ABA-Fe_3O_4 in the C–C coupling reaction, we first examined the reaction between 4-nitrobromobenzene and sodium tetraphenyl borate, and the results are summarized in Table 1. In order to optimize reaction conditions, we examined different parameters such as solvent, base, reaction temperature and different amounts of Pd(0)-ABA-Fe_3O_4, on the outcome of C–C coupling reaction of 4-nitrobromobenzene and sodium tetraphenyl borate. The catalyst is not thermal, air or moisture sensitive, and hence, inert atmosphere was not employed. It is very important that the reaction did not proceed in the absence of Pd(0)-ABA-Fe_3O_4 even after long time (Table 1, entry 1). In order to choose the reaction media, different solvents such as PEG, DMF, DMSO, H_2O

Table 1 Optimization of reaction conditions for the C–C coupling reaction of 4-nitrobromobenzene with sodium tetraphenyl borate

Entry	Catalyst (mg)	Solvent	Base	Temperature (°C)	Time (min)	Yield (%)[a]
1	–	PEG	Na_2CO_3	80	300	–[b]
2	5	PEG	Na_2CO_3	80	120	97
3	7	PEG	Na_2CO_3	80	90	98
4	10	PEG	Na_2CO_3	80	40	97
5	15	PEG	Na_2CO_3	80	30	98
6	10	DMF	Na_2CO_3	80	40	42
7	10	H_2O	Na_2CO_3	80	40	17
8	10	DMSO	Na_2CO_3	80	120	Trace
9	10	Dioxane	Na_2CO_3	80	120	Trace
10	10	PEG	NaOH	80	40	24
11	10	PEG	NaOEt	80	120	Trace
12	10	PEG	KOH	80	120	31
13	10	PEG	Et_3N	80	40	18
14	10	PEG	Na_2CO_3	60	120	57
15	10	PEG	Na_2CO_3	40	120	Trace
16	10	PEG	Na_2CO_3	R.t.	120	–[b]

[a] Isolated yield

[b] No reaction

and dioxane were used (Table 1, entries 6–9) and the best results were obtained in PEG using 0.01 g (1.85 mol%) of Pd(0)-ABA-Fe_3O_4 (Table 1, entry 4). Also, the effect of base was studied in which inferior results were obtained using NaOH, NaOEt, KOH and Et_3N (Table 1, entries 10–13). But, when Na_2CO_3 was used (Table 1, entry 4), excellent biphenyl yields were obtained. Also, we found that the coupling reaction yields were susceptible to temperature changes. Therefore, the effect of temperature was described (Table 1, entries 14–16) and the best results were obtained at 80 °C. As listed in Table 1, 4-nitrobromobenzene (1 mmol) in the presence of catalytic amount of Pd(0)-ABA-Fe_3O_4 (0.01 g, 1.85 mol%) using sodium tetraphenyl borate (0.5 mmol) and Na_2CO_3 (3 mmol) in PEG at 80 °C was found to be ideal in the reaction conditions for the formation of corresponding biphenyl.

With the above-mentioned reaction conditions in hand, we examined the catalytic activity of Pd(0)-ABA-Fe_3O_4 for various substrates, and the results are given in Table 2. Thus, various ortho-, metha- and para-substituted aryl iodides (Table 2, entries 1–6) and bromides (Table 2, entries 7–13) were coupled into corresponding biphenyls. We also examined the reaction with several substituted aryl chlorides (Table 2, entries 14–16) and sodium tetraphenyl borate under the optimized reaction conditions. Therefore, the Pd(0)-ABA-Fe_3O_4 catalyst was also capable of chlorobenzene derivatives. However, the completing reaction including aryl chlorides was slower and required more amounts of catalyst (20 mg, 3.7 mol%) than aryl iodides and bromides. In order to show the chemoselectivity of the presented protocol, 1-chloro-4-bromobenzene was subjected to the C–C coupling reaction. Interestingly, chloro-group remained intact during the coupling reaction, while the bromo-group was coupled successfully (Table 2, entry 12). The experimental procedure is very simple and convenient and has the ability to tolerate a variety of other functional groups such as OH, CN, NO_2, alkyl and OCH_3 under the reaction conditions. Therefore, the results revealed that this methodology is effective for a wide range of aryl halide including Cl, Br and I; however, aryl chlorides showed less reactivity toward the coupling reaction than their aryl iodides and bromides analogs.

Also, we report the application of Pd(0)-ABA-Fe_3O_4 as catalyst for the Suzuki reaction using the coupling of various aryl halides with phenylboronic acid (Scheme 3). In order to optimize the reaction conditions, the coupling of iodobenzene (1 mmol) with $PhB(OH)_2$ (1 mmol) was optimized in the presence of different amounts of catalyst (Table 3, entries 1–5) and in the various solvents such as H_2O, EtOH, DMSO, PEG and DMF (Table 3, entries 5–9). The reaction was significantly affected by the nature of base and the additive used. Therefore, to found the best reaction condition, the effect and amount of base were described (Table 3, entries 9–14) and the best results were obtained using 3 mmol of triethylamine (Et_3N). When the amount of Et_3N was reduced to 1.5 mmol, the yield of the reaction decreased to 54%. Therefore, the best results were obtained in water at room temperature for 45 min in the presence of 3 mg (0.56 mol%) of catalyst using 3 mmol of Et_3N (Table 3, entry 4).

After the optimization of the reaction condition, the various aryl halides including several of functional groups

Table 2 Catalytic C–C coupling reaction of aryl halides using $NaBPh_4$ in the presence of catalytic amounts of Pd(0)-ABA-Fe_3O_4 in PEG at 80 °C

Entry	Aryl halide	Time (min)	Yield (%)[a]	Melting point (°C) [ref.]
1	Iodobenzene	65	94	65–66 [38]
2	1-Iodonaphthalene	250	87	Oil [39]
3	4-Iodotoluene	200	98	42–44 [38]
4	4-Iodoanisole	180	99	82–84 [38]
5	2-Iodotoluene	240	90	Oil [40]
6	2-Iodoanisole	150	89	Oil [41]
7	4-Bromotoluene	40	94	42–43 [38]
8	4-Bromophenol	40	98	160–162 [39]
9	Bromobenzene	50	95	64–66 [38]
10	4-Bromonitrobenzene	40	97	111–112 [38]
11	4-Bromobenzonitrile	30	98	82–83 [39]
12	4-Bromochlorobenzene	20	98	71–73 [38]
13	3-Bromopyridine	90	90	Oil [40]
14	4-Chloronitrobenzene	25	97[b]	111–113 [38]
15	4-Chlorobenzonitrile	200	91[b]	83–85 [39]
16	Chlorobenzene	80	93[b]	64–66 [38]

[a] Isolated yield

[b] *Reaction conditions* aryl halide (1 mmol), Pd(0)-ABA-Fe_3O_4 (20 mg, 3.7 mol%), sodium tetraphenyl borate (0.5 mml) and Na_2CO_3 (3 mmol) in PEG at 80 °C

Scheme 3 Pd(0)-ABA-Fe_3O_4 catalyzed the Suzuki reaction

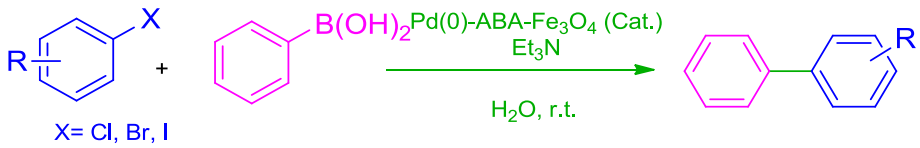

have been described in optimum condition and the corresponding biphenyl were obtained in short reaction times with good to excellent yields (Table 4). The experimental procedure is very simple, and also a variety of aryl halides (involving of Cl, Br and I) possessing of electron-donor and electron-withdrawing substituents were successfully employed to prepare the corresponding biphenyl derivatives in excellent yields at room temperature. Aryl bromides and aryl iodides show lower reaction times compared to those corresponding aryl chlorides (Table 4, entries 5–8).

To extend the scope of our work, we next investigated the Heck reaction using coupling of various aryl halides with butyl acrylate, styrene and acrylonitrile (Scheme 4).

The reaction conditions, such as solvent (DMF, DMSO or PEG), base (Et_3N, Na_2CO_3 or K_2CO_3) and amount of catalyst, were optimized in the coupling of iodobenzene with butyl acrylate as model reaction (Table 5). Also, the effect of temperature was studied, in which inferior results were obtained in 80 and 100 °C (Table 5, entries 9, 10).

As given in Table 5, the best result was obtained with the use of K_2CO_3 as the base and DMF as the solvent in the presence of 8 mg (1.48 mol%) of Pd(0)-ABA-Fe_3O_4 at 120 °C (Table 5, entry 3). When the same reaction

Table 3 Optimization of reaction conditions for the coupling of iodobenzene (1 mmol) with $PhB(OH)_2$ (1 mmol) for 45 min at room temperature

Entry	Catalyst (mg)	Solvent	Base	Amounts of base (mmol)	Yield (%)[a]
1	–	H_2O	Et_3N	3	–[b]
2	1	H_2O	Et_3N	3	45
3	2	H_2O	Et_3N	3	75
4	3	H_2O	Et_3N	3	98
5	5	H_2O	Et_3N	3	98[c]
6	3	PEG	Et_3N	3	–[d]
7	3	DMF	Et_3N	3	–[d]
8	3	DMSO	Et_3N	3	–[d]
9	3	EtOH	Et_3N	3	–[d]
10	3	H_2O	Na_2CO_3	3	50
11	3	H_2O	NaOEt	3	Trace
12	3	H_2O	Na_2SO_4	3	48
13	3	H_2O	NaOH	3	59
14	3	H_2O	Et_3N	1.5	54

[a] Isolated yield

[b] No reaction after 24 h

[c] The reaction time is 20 min

[d] No reaction after 120 min

Table 4 Coupling of aryl halides with $PhB(OH)_2$ in the presence of catalytic amounts of Pd(0)-ABA-Fe_3O_4 in water at room temperature

Entry	Aryl halide	Time (min)	Yield (%)[a]	Melting point (°C) [Ref.]
1	Iodobenzene	45	98	64–66 [38]
2	4-Iodotoluene	180	96	42–43 [38]
3	4-Iodoanisole	195	95	81–83 [38]
4	4-Bromotoluene	135	98	42–43 [38]
5	4-Bromochlorobenzene	45	97	70–72 [38]
6	1-Bromo-3-(trifluoromethyl) benzene	25	97	Oil [40]
7	4-Bromonitrobenzene	50	98	112–115 [52]
8	Bromobenzene	55	98	63–65 [38]
9	4-Chloronitrobenzene	120	96	112–113 [52]
10	Chlorobenzene	145	97	64–66 [38]

[a] Isolated yield

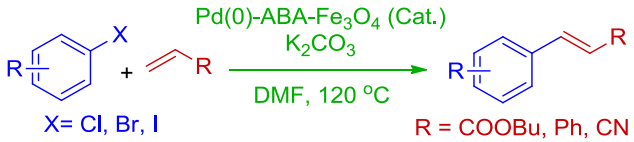

Scheme 4 Pd(0)-ABA-Fe_3O_4 catalyzed the Heck reaction

Table 5 Optimization of reaction conditions for the C–C coupling reaction of iodobenzene with butyl acrylate for 25 min

Entry	Catalyst (mg)	Solvent	Base	Temperature (°C)	Yield (%)[a]
1	–	DMF	K_2CO_3	120	–[b]
2	5	DMF	K_2CO_3	120	65
3	8	DMF	K_2CO_3	120	98
4	10	DMF	K_2CO_3	120	98[c]
5	8	PEG	K_2CO_3	120	50
6	8	DMSO	K_2CO_3	120	75
7	8	DMF	Na_2CO_3	120	60
8	8	DMF	Et_3N	120	70
9	8	DMF	K_2CO_3	100	38
10	8	DMF	K_2CO_3	80	25

[a] Isolated yield

[b] No reaction after 24 h

[c] The reaction time is 15 min

was tested at 100 °C, the reaction yield increased to 38% (Table 5, entry 9).

The best conditions were then applied to coupling of other aryl halides (including Cl, Br and I) with butyl acrylate in a short reaction times (Table 6). As listed in Table 6, aryl bromides and aryl iodides underwent the Heck reaction with butyl acrylate under similar conditions to afford the corresponding products in 95–98% yields (Table 6, entries 1–9), whereas aryl chlorides such as chlorobenzene and 4-chlorobenzonitrile have been coupled with butyl acrylate in the presence of 16 mg (2.96 mol%) of Pd(0)-ABA-Fe_3O_4 in 97 and 96% yields, respectively (Table 6, entries 10, 11). Aryl halides with electron-donor (Table 6, entries 2–5) and electron-withdrawing (Table 6, entries 7–10) functional groups reacted with butyl acrylate to afford the corresponding products and the all products were obtained in good to excellent yields.

We also applied optimized reaction conditions to coupling aryl halides with acrylonitrile and styrene (Table 6, entries 12–22). The electron-neutral, electron-rich and electron-poor aryl halides reacted with acrylonitrile and styrene efficiently to produce the corresponding cross-coupling products in good to excellent yields, whereas styrene has been coupled with aryl halides in the presence of 16 mg (2.96 mol%) of Pd(0)-ABA-Fe_3O_4 in 68–80% yields. Therefore, these results revealed that this methodology is effective for a wide range of alkenes and aryl halides.

In order to extend applications of the catalytic activity of Pd(0)-ABA-Fe_3O_4, this catalyst was investigated in the direct amination of aryl iodides and aryl bromides using aqueous ammonia (Scheme 5).

The Pd(0)-ABA-Fe_3O_4 has been tested as catalyst in the amination of iodobenzene using ammonia solution to ascertain the most optimum conditions. The effect of solvent, base, temperature and amounts of catalyst on the outcome of the amination of iodobenzene was examined. A summary of the results is given in Table 7. The reaction did not perform in the absence of Pd(0)-ABA-Fe_3O_4 or base (Table 7, entries 4, 10). As given in Table 7, the best result was obtained with the use of K_2CO_3 (3 mmol) in the presence of 10 mg (1.85 mol%) of Pd(0)-ABA-Fe_3O_4 at 60 °C under solvent-free conditions.

This optimized reaction conditions were then applied to direct amination of electron-poor or electron-rich aryl iodides or bromides using aqueous ammonia to give

Table 6 Coupling of aryl halides with butyl acrylate, acrylonitrile or styrene (Heck reaction) in the presence of catalytic amounts of Pd(0)-ABA-Fe_3O_4

Entry	Aryl halide	Alkene	Time (min)	Yield (%)[a]	Melting point (°C) [ref.]
1	Iodobenzene	Butyl acrylate	25	98	Oil [45]
2	4-Iodotoluene	Butyl acrylate	35	97	Oil [46]
3	4-Iodoanisole	Butyl acrylate	45	98	Oil [45]
4	2-Iodotoluene	Butyl acrylate	450	94	Oil [47]
5	2-Iodoanisole	Butyl acrylate	380	98	Oil [48]
6	Bromobenzene	Butyl acrylate	90	95	Oil [46]
7	3-Bromopyridine	Butyl acrylate	15	98	Oil [46]
8	4-Bromochlorobenzene	Butyl acrylate	720	97	Oil [46]
9	4-Bromobenzonitrile	Butyl acrylate	480	97	39–42 [46]
10	4-Chlorobenzonitrile	Butyl acrylate	20 h	96[b]	39–42 [46]
11	Chlorobenzene	Butyl acrylate	540	97[b]	Oil [47]
12	Iodobenzene	Styrene	15 h	80[b]	124–126 [49]
13	4-Iodotoluene	Styrene	15 h	76[b]	120–122 [50]
14	4-Iodoanisole	Styrene	15 h	71[b]	135–137 [49]
15	Bromobenzene	Styrene	15 h	75[b]	123–125 [49]
16	4-Bromonitrobenzene	Styrene	15 h	68[b]	158–160 [49]
17	Iodobenzene	Acrylonitrile	165	96	Oil [50]
18	4-Iodotoluene	Acrylonitrile	205	96	70–73 [51]
19	4-Bromotoluene	Acrylonitrile	315	95	70–73 [52]
20	2-Iodotoluene	Acrylonitrile	600	97	Oil
21	Bromobenzene	Acrylonitrile	300	97	Oil [53]
22	Chlorobenzene	Acrylonitrile	480	95	Oil [50]

[a] Isolated yield

[b] *Reaction conditions* aryl halide (1 mmol), Pd(0)-ABA-Fe_3O_4 (16 mg, 2.96 mol%), alkene (1.2 mmol) and K_2CO_3 (3 mmol) in DMF at 120 °C

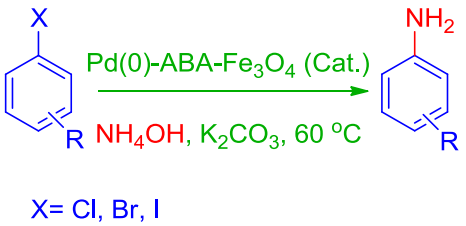

Scheme 5 Pd(0)-ABA-Fe_3O_4 catalyzed the amination of aryl halides

aniline derivatives (Table 8). In all cases, the products were resulted in good yield.

Reusability of the catalyst

The Pd(0)-ABA-Fe_3O_4 as magnetically nanocatalyst can be easily recycled for repeatedly C–C coupling reaction. To investigate this issue, the recyclability of the catalyst was examined for the coupling reaction of 4-nitrobromobenzene with phenylboronic acid and sodium tetraphenyl borate. We found that this catalyst demonstrated remarkably excellent reusability; after the completion of the reaction, the catalyst was easily and rapidly recovered from the reaction mixture using an external magnet, the remaining

Table 7 Optimization of the reaction conditions for the amination of iodobenzene in 6 h

Entry	Catalyst (mg)	Solvent	Base	Temperature (°C)	Yield (%)[a]
1	10	H_2O	K_2CO_3	60	54
2	10	DMF	K_2CO_3	60	65
3	10	EtOH	K_2CO_3	60	36
4	–	Solvent free	K_2CO_3	60	–[b]
5	5	Solvent free	K_2CO_3	60	63
6	10	Solvent free	K_2CO_3	60	94
7	10	Solvent free	Na_2CO_3	60	83
8	10	Solvent free	KOH	60	40
9	10	Solvent free	Et_3N	60	88
10	10	Solvent free	–	60	–[b]
11	10	Solvent free	K_2CO_3	40	31

[a] Isolated yield

[b] No reaction after 10 h

Table 8 Amination of aryl halides in the presence of Pd(0)-ABA-Fe_3O_4 using aqueous ammonia

Entry	Aryl halide	Product	Time (h)	Yield (%)[a]	Melting point (°C)
1	Iodobenzene	Aniline	6	94	Oil [27]
2	Bromobenzene	Aniline	8	92	Oil [27]
3	4-Bromochlorobenzene	4-Chloroaniline	10	90	68–70 [54]
4	4-Iodotoluene	*p*-Toluidine	5	94	43–44 [27]
5	4-Iodoanisole	4-Methoxyaniline	7	92	56–58 [54]
6	1-Bromonaphthalene	Naphthalen-1-amine	40	91	47–49 [27]
7	4-Bromonitrobenzene	4-Nitroaniline	5	95	145–148 [54]
8	2-Bromopyridine	Pyridin-2-amine	7	96	54–58 [55]
9	4-Bromophenol	4-Aminophenol	14	94	185–190 [55]
10	4-Bromobenzonitrile	4-Aminobenzonitrile	5.5	93	87–88 [27]

[a] Isolated yield

magnetic nanocatalyst was washed with diethyl ether to remove residual product and the reaction mixture decanted. Then, the reaction vessel was charged with fresh substrates and subjected to the next run. As shown in Fig. 8, the catalyst was used over five runs without any significant loss of its activity. The average isolated yield for five successive runs was 93 and 95%, which clearly demonstrates the practical recyclability of this catalyst. In addition, one of the attractive features of this catalytic system is the rapid and efficient separation of the catalyst using an appropriate external magnet, which minimizes the loss of catalyst during separation.

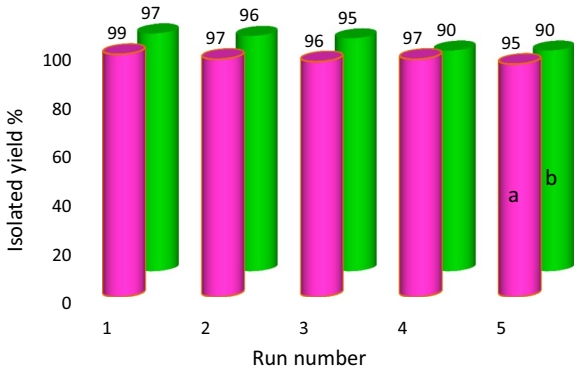

Fig. 8 Recyclability of Pd(0)-ABA-Fe_3O_4 in the: [a]coupling of 4-nitrobromobenzene (1 mmol) with $NaBPh_4$ (0.5 mmol) at 80 °C in PEG and [b]coupling of 4-nitrobromobenzene (1 mmol) with $PhB(OH)_2$ (1 mmol) at room temperature in H_2O. Reusability of the nanocatalyst

Catalyst leaching study

In order to examine leaching of palladium in reaction mixture and heterogeneity of described catalyst, we performed hot filtration for the synthesis of biphenyl with tetraphenyl borate. In this experiment, we obtained the yield of product in half time of the reaction that it was 56%. Then, the reaction was repeated and in half time of the reaction, the catalyst separated and allowed the filtrate to react further. We found that, after this hot filtration, no further reaction was observed. The yield of reaction in this stage was 57% that confirmed the leaching of palladium is negligible.

Also, to extend the analysis of leaching of catalyst, amount of Pd in Pd(0)-ABA-Fe_3O_4 was determined by ICP-OES after five times recycled. The amount of Pd in catalysts was found to be 1.81×10^{-3} mol g^{-1} based on ICP-OES for catalyst after five runs reused. Therefore, the catalyst can be recovered and reused without any significant loss of amount of Pd leaching. Based on ICP-OES results, amount of Pd in the catalyst after 5 times reused is comparable with fresh catalyst (1.85×10^{-3} mol g^{-1} for fresh Pd(0)-ABA-Fe_3O_4). Therefore, only 2% leaching of catalyst was observed after five runs.

Comparison of the catalyst

In order to examine the efficiency of these procedures, we compared the results of the coupling of iodobenzene with phenylboronic acid (Table 9) with the previous methods in the literature. This catalyst showed short reaction time and good yield than other catalysts reported in the previous literatures. Also, this new catalyst is comparable in terms of price, non-toxicity, stability and easy separation. In addition, the recovered and recycled of this catalyst is more rapid and easier than the other catalysts.

Conclusions

In conclusion, an efficient heterogeneous catalyst (Pd(0)-ABA-Fe_3O_4) was synthesized from loading palladium acetate onto functionalized Fe_3O_4 nanoparticles. The

Table 9 Comparison results of Pd(0)-ABA-Fe_3O_4 with other catalysts for the coupling of iodobenzene with phenylboronic acid

Entry	Catalyst (mol% of Pd)	Condition	Time (min)	Yield (%)	Ref.
1	Pd NP (1.0 mol%)	H_2O, KOH, 100 °C	12 h	95	[41]
2	CA/Pd(0) (0.5–2.0 mol%)	H_2O, K_2CO_3, 100 °C	120	94	[42]
3	$PdCl_2$ (0.05 mol%)	DMF, Cs_2CO_3, 130 °C	120	95	[43]
4	Pd/Au NPs (4.0 mol%)	EtOH/H_2O, K_2CO_3, 80 °C	24 h	88	[44]
5	NHC-Pd(II) complex (1.0 mol%)	THF, Cs_2CO_3, 80 °C	12 h	88	[45]
6	Pd(II)–NHC complex (1 mol%)	DMF, Cs_2CO_3, 100 °C	24 h	99	[47]
7	*N*,*N*′-bis(2-pyridinecarboxamide)-1,2-benzene palladium complex (1 mol%)	H_2O, K_2CO_3, 100 °C	180	97	[56]
8	PANI-Pd (2.2 mol%)	K_2CO_3, 1,4-dioxane: H_2O (1:1), 95 °C	4 h	91	[57]
9	Pd(0)-ABA-Fe_3O_4 (0.56 mol%)	H_2O, Et_3N, r.t.	45	98	This work

Pd(0)-ABA-Fe_3O_4 nanoparticles exhibit an excellent catalytic activity, high reusability and air or moisture stability for the Heck and Suzuki reactions also amination of aryl halides. This methodology is effective for a wide range of aryl halide including Cl, Br and I. A high conversion of the substrates was obtained in C–C coupling reaction using sodium tetraphenyl borate, phenylboronic acid, styrene, acrylonitrile and butyl acrylate in the presence of this catalyst. The advantages of this protocol are the use of a commercially available, eco-friendly, cheap, chemically stable materials, the operational simplicity, practicability and good to high yields, and more importance the catalyst can be synthesized readily from inexpensive and commercially available starting materials. Also, the all reactions were carried out in air atmosphere.

Acknowledgements This work was supported by the research facilities of Ilam University, Ilam, Iran.

References

1. S. Das, S. Bhunia, T. Maity, S. Koner, J. Mol. Catal. A Chem. **394**, 188 (2014)
2. M. Wena, S. Takakura, K. Fuku, K. Moria, H. Yamashita, Catal. Today **242**, 381 (2015)
3. S. Kazemi Movahed, R. Esmatpoursalmani, A. Bazgir, RSC Adv. **4**, 14586 (2014)
4. N. Miyaura, A. Suzuki, Chem. Rev. **95**, 2457 (1995)
5. G. Herve, G. Sartori, G. Enderlin, G. Mackenzie, C. Len, RSC Adv. **4**, 18558 (2014)
6. D.A. Alonso, C. Najera, Chem. Soc. Rev. **39**, 2891 (2010)
7. X. Le, Z. Dong, Z. Jin, Q. Wang, J. Ma, Catal. Commun. **53**, 47 (2014)
8. D. Zhang, Q. Wang, Coord. Chem. Rev. **286**, 1 (2015)
9. A. Ghorbani-Choghamarani, P. Moradi, B. Tahmasbi, RSC Adv. **6**, 56638 (2016)
10. A. Ghorbani-Choghamarani, B. Tahmasbi, P. Moradi, N. Havasi, Appl. Organomet. Chem. **30**, 619 (2016)
11. M. Opanasenko, P. Stepnicka, J. Cejka, RSC Adv. **4**, 65137 (2014)
12. P. Sharma, A.P. Singh, Catal. Sci. Technol. **4**, 2978 (2014)
13. S.S. Soni, D.A. Kotadia, Catal. Sci. Technol. **4**, 510 (2014)
14. M.M. Heravi, S. Sadjadi, J. Iran. Chem. Soc. **6**, 1 (2009)
15. P. Nehra, B. Khungar, K. Pericherla, S.C. Sivasubramanian, A. Kumar, Green Chem. **16**, 4266 (2014)
16. P.M. Uberman, L.A. Perez, S.E. Martın, G.I. Lacconi, RSC Adv. **4**, 12330 (2014)
17. M. Gholinejad, B. Karimi, F. Mansouri, J. Mol. Catal. A Chem. **386**, 20 (2014)
18. B. Atashkar, A. Rostami, B. Tahmasbi, Catal. Sci. Technol. **3**, 2140 (2013)
19. R.K. Sharma, M. Yadav, R. Gaur, Y. Monga, A. Adholeya, Catal. Sci. Technol. **5**, 2728 (2015)
20. V. Polshettiwar, R. Luque, A. Fihri, H. Zhu, M. Bouhrara, J.M. Basset, Chem. Rev. **111**, 3036 (2011)
21. B. Atashkar, A. Rostami, H. Gholami, B. Tahmasbi, Res. Chem. Intermed. **41**, 3675 (2015)
22. A. Rostami, B. Tahmasbi, A. Yari, Bull. Korean Chem. Soc. **34**, 1521 (2013)
23. C.W. Lim, I.S. Lee, Nano Today **5**, 412 (2010)
24. K. Kulkarni, J. Friend, L. Yeo, P. Perlmutter, Ultrason. Sonochem. **21**, 1305 (2014)
25. T. Yu, X.Y. Wu, J. Yang, Tetrahedron Lett. **55**, 4071 (2014)
26. R.B. Nasir Baig, R.S. Varma, RSC Adv. **4**, 6568 (2014)
27. F. Havasi, A. Ghorbani-Choghamarani, F. Nikpour, N. J. Chem. **39**, 6504 (2015)
28. R.A. Green, J.F. Hartwig, Angew. Chem. Int. Ed. **54**, 1 (2015)
29. B. Yang, L. Liao, Y. Zeng, X. Zhu, Y. Wan, Catal. Commun. **45**, 100 (2014)
30. J. Li, L. Liu, RSC Adv. **2**, 10485 (2012)
31. A. Ghorbani-Choghamarani, Z. Darvishnejad, B. Tahmasbi, Inorg. Chim. Acta **435**, 223 (2015)
32. M. Hajjami, B. Tahmasbi, RSC Adv. **5**, 59194 (2015)
33. W. Zhang, X. Chen, T. Tang, E. Mijowska, Nanoscale **6**, 12884 (2014)
34. M. Nikoorazm, A. Ghorbani-Choghamarani, M. Khanmoradi, Appl. Organomet. Chem. **30**, 236 (2016)
35. A. Ghorbani-Choghamarani, M. Hajjami, B. Tahmasbi, N. Noori, J. Iran. Chem. Soc. **13**, 2193 (2016)
36. A. Ghorbani-Choghamarani, B. Tahmasbi, F. Arghand, S. Faryadi, RSC Adv. **5**, 92174 (2015)
37. A. Ghorbani-Choghamarani, B. Tahmasbi, N. J. Chem. **40**, 1205 (2016)
38. Y.Y. Peng, J. Liu, X. Lei, Z. Yin, Green Chem. **12**, 1072 (2010)
39. L. Baia, J.X. Wanga, Adv. Synth. Catal. **350**, 315 (2007)

40. X. Zheng, Q. Yang, Z. Li, Z. Zhu, X. Cui, H. Fu, H. Chen, R. Li, Catal. Commun. **57**, 143 (2014)
41. M. Nasrollahzadeh, S.M. Sajadi, M. Maham, J. Mol. Catal. A: Chem. **396**, 297 (2015)
42. V.W. Faria, D.G.M. Oliveira, M.H.S. Kurz, F.F. Goncalves, C.W. Scheeren, G.R. Rosa, RSC Adv. **4**, 13446 (2014)
43. S.J. Sabounchei, A. Hashemi, Inorg. Chem. Commun. **47**, 123 (2014)
44. M. Nasrollahzadeh, A. Azarian, M. Maham, A. Ehsani, J. Ind. Eng. Chem. **21**, 746 (2015)
45. T. Chen, J. Gao, M. Shi, Tetrahedron **62**, 6289 (2006)
46. N. Iranpoor, H. Firouzabadi, A. Tarassoli, M. Fereidoonnezhad, Tetrahedron **66**, 2415 (2010)
47. Q. Xu, W.L. Duan, Z.Y. Lei, Z.B. Zhu, M. Shi, Tetrahedron **61**, 11225 (2005)
48. Y.P. Wang, H.M. Lee, J. Organomet. Chem. **791**, 90 (2015)
49. Q. Du, W. Zhang, H. Ma, J. Zheng, B. Zhou, Y. Li, Tetrahedron **68**, 3577 (2012)
50. Y. Leng, F. Yang, K. Wei, Y. Wu, Tetrahedron **66**, 1244 (2010)
51. L. Wang, H. Li, P. Li, Tetrahedron **65**, 364 (2009)
52. A. Ghorbani-Choghamarani, B. Tahmasbi, P. Moradi, RSC Adv. **6**, 43205 (2016)
53. A. Ghorbani-Choghamarani, B. Tahmasbi, P. Moradi, Appl. Organomet. Chem. **30**, 422 (2016)
54. K.G. Thakur, K.S. Srinivas, K. Chiranjeevi, G. Sekar, Green Chem. **13**, 2326 (2011)
55. M. Nikoorazm, A. Ghorbani-Choghamarani, N. Noori, B. Tahmasbi, Appl. Organomet. Chem. **30**, 843 (2016)
56. M. Gholinejad, H.R. Shahsavari, Inorg. Chim. Acta **421**, 433 (2014)
57. H.A. Patel, A.L. Patel, A.V. Bedekar, Appl. Organomet. Chem. **29**, 1 (2015)